Int. J. Morphol.,
44(3):756-765, 2026.

http://dx.doi.org/10.4067/s0717-95022026000300756

Mandibular Strength and Trabecular Morphology in Hyperglycemic Rabbits Under Zinc and Insulin Therapy

Resistencia Mandibular y Morfología Trabecular en Conejos Hiperglucémicos Bajo Tratamiento con Zinc e Insulina

Olufemi Ogundipe[1,3]; Vaughan Perry[2]; Nhlanhla Lucky Japhta[2]; Diana Pillay[2] & Robert Ndou[2]

OGUNDIPE, O.; PERRY, V.; JAPHTA, N.L.; PILLAY, D. & NDOU, *R.* Mandibular strength and trabecular morphology in hyperglycemic rabbits under zinc and insulin therapy. *Int. J. Morphol., 44(3)*:756-765, 2026.

SUMMARY: Diabetic complications arise primarily from chronic hyperglycemia, a hallmark of the disease that is becoming increasingly prevalent worldwide. Among these complications, skeletal involvement remains one of the least studied. This study aimed to evaluate the impact of sustained hyperglycemia and therapeutic interventions with zinc and insulin on mandibular bone strength and microarchitecture using an alloxan-induced rabbit model. Fifty male rabbits were randomly assigned to five groups: untreated control (UN), hyperglycemic untreated (HG), hyperglycemic zinc-treated (HG+Zn), hyperglycemic insulin-treated (HG+Ins), and hyperglycemic zinc-plus-insulin-treated (HG+Zn+Ins). Diabetes was induced with alloxan, and treatments were administered for 12 weeks. The right hemimandible was analysed using high-resolution micro-computed tomography (Micro-CT) and biomechanical testing. Morphometric parameters (BV/TV, TbTh, TbN, TbSp, CtTh) and mechanical strength properties were compared across groups. Hyperglycemia significantly reduced bone volume fraction and cortical thickness, confirming mandibular vulnerability to diabetic osteopathy. Maximum force did not differ significantly among groups. Yield point analysis revealed increased stiffness and brittleness in HG and HG+Zn groups, while insulin therapy normalized yield point values. Zinc monotherapy failed to prevent microarchitectural deterioration, and combined zinc-insulin therapy unexpectedly impaired trabecular integrity, suggesting a negative pharmacological interaction. Persistent cortical thinning across all hyperglycemic groups indicates irreversible structural deficits despite treatment. Insulin is essential for preserving trabecular bone and restoring material properties compromised by hyperglycemia, whereas zinc alone offers no protective effect. The lack of synergy between zinc and insulin shows the need for optimization of combined therapies. Early and stringent glycemic control remains critical to prevent irreversible skeletal damage.

KEY WORDS: Diabetes mellitus; Hyperglycemia; Mandible; Zinc; Insulin; Bone.

INTRODUCTION

Diabetes mellitus has become a global epidemic, with alarmingly rising prevalence rates imposing a substantial burden on healthcare systems (Sun *et al*., 2022). The defining pathophysiological feature of diabetes mellitus is chronic hyperglycemia, resulting from defects in insulin secretion, insulin action, or both (Adeghate *et al*., 2006). Although hyperglycemia is the central systemic characteristic, the complications of diabetes extend beyond glycaemic control. Among the debilitating yet frequently overlooked complications is diabetic skeletopathy, which is characterised by deterioration of skeletal integrity (Costantini & Conte 2019) including the craniofacial skeleton (Hendrijantini *et al*., 2023).

The mandible constitutes a biomechanically critical component of the craniofacial skeleton, functioning as a primary load-bearing structure essential for mastication, phonation, and maintenance of facial morphology. Its structural integrity is therefore indispensable for optimal oral function. In the context of diabetes mellitus, pathological alterations in mandibular bone quality have been implicated in heightened susceptibility to periodontal disease, impaired osseous healing following maxillofacial interventions, and markedly increased rates of dental implant failure (Abbassy *et al*., 2010).

Elucidating the mechanism underlying these clinical failures is complicated by the 'diabetic bone paradox'. In particular in type 2 diabetes mellitus, patients often present with normal or elevated bone mineral density yet paradoxically experience increased bone fragility and

[1] School of Anatomical Sciences, Faculty of Health Sciences, University of Witwatersrand, Johannesburg, South Africa.
[2] Department of Human Anatomy and Histology, School of Medicine, Sefako Makgatho Health Sciences University, Pretoria, South Africa.
[3] Department of Oral and Maxillofacial Surgery and Oral Pathology, Faculty of Dentistry, Obafemi Awolowo University, Ile-Ife, Nigeria.

Received: 2026-01-07 Accepted: 2026-03-28

implant failure. This indicates that the diabetic skeletal defect involves not only a loss of mass, but a profound degradation of bone quality, which encompasses microarchitecture, collagen maturity, and mineralisation (Sharma *et al*., 2024). Although type 1 diabetes mellitus typically presents with classical cortical thinning and porosity the overall consensus is that diabetes, regardless of type, induces a state of biomechanically incompetent bone (Walle *et al*., 2022). However, the specific manifestation of this incompetence in the mandible is not fully elucidated.

The pathophysiological basis of this impairment is rooted in a profound disruption of bone remodelling dynamics. Chronic hyperglycemia exerts a dual effect on skeletal turnover by directly inhibiting osteoblastogenesis while simultaneously potentiating osteoclastic resorption, thus skewing the balance toward net bone loss (Dlamini & Ndou, 2023). Complementing this, insulin deficiency, a defining feature of type 1 diabetes and advanced type 2 diabetes, eliminates a critical anabolic stimulus for osteoblast activity, further exacerbating skeletal deterioration (Thrailkill *et al*., 2005). Although conventional insulin therapy remains indispensable for glycaemic regulation and survival, accumulating evidence indicates that insulin monotherapy is insufficient to fully reverse established deficits in bone microarchitecture or restore the integrity of the organic matrix (Wu *et al*., 2022).

This therapeutic limitation underscores the need for adjunctive interventions targeting downstream molecular pathways of bone metabolism. Zinc, an essential trace element, has emerged as a biologically plausible candidate as it fulfils multiple roles in skeletal physiology. It functions as a cofactor for alkaline phosphatase, a pivotal enzyme in mineralisation, stabilizes collagen fibrillogenesis, and exhibits antioxidant properties (Molenda & Kolmas, 2023). Despite these theoretical advantages, the capacity of zinc to attenuate mandibular osteopathy and, more critically, its potential to act synergistically with insulin to restore biomechanical competence remains an unresolved and clinically significant question.

Most existing investigations into diabetic bone pathology have focused predominantly on appendicular skeletal sites such as the tibia and femur (Park *et al*., 2013). However, extrapolating these findings to the mandible is biologically inappropriate due to fundamental differences in embryological origin and ossification mechanisms. Long bones arise from the lateral plate mesoderm and undergo endochondral ossification, whereas the mandibular body is derived from cranial neural crest cells and forms primarily through intramembranous ossification (Lee *et al*., 2001). These divergent developmental lineages confer distinct osteogenic capacities, remodelling kinetics, and molecular signaling profiles under metabolic stress (Leucht *et al*., 2008). Consequently, the therapeutic responsiveness of neural crest–derived mandibular bone to agents such as insulin and zinc represents a discrete biological question that cannot be resolved through studies confined to the appendicular skeleton. To address this critical knowledge gap, the present study uses a controlled insulinopenic rabbit model to minimise systemic confounders and takes advantage of high-resolution microcomputed tomography (Micro-CT) alongside biomechanical testing to deliver a hierarchical evaluation of mandibular bone quality.

MATERIAL AND METHOD

All protocols, procedures and experiments described were approved by the Animal Research and Ethics Committee of Obafemi Awolowo University, Ile-Ife, Osun State, Nigeria (IPH/OAU/12/1224).

Rabbits

Healthy male rabbits (n=50), approximately six months old (180–194 days) and weighing 1300–2900 g, were sourced from a local farm in Ile-Ife, Nigeria. They were housed under specific pathogen-free conditions in the Multidisciplinary Laboratory for Animal Administration at Obafemi Awolowo University, with controlled temperature (21–23 °C) and a 12-hour light/dark cycle. Each rabbit was kept individually in a well-ventilated metal cage (1.2 m × 0.6 m) that allowed free movement. Before the study began, all animals underwent a two-week acclimatization period.

Grouping of rabbits and Zinc supplementation and insulin therapy

After successfully inducing diabetes, the rabbits were randomly assigned into 5 groups of 10 rabbits each as per the treatment group using a computer-generated number sampling technique. The treatment groups comprised of: (i) untreated control (UN), and hyperglycemia induced experimental groups namely; (ii) hyperglycemia untreated control (HG), (iii) hyperglycemia zinc treated (HG+Zn), (iv) hyperglycemia Insulin treated (HG+Ins) and (v) hyperglycemia Zinc and Insulin treated groups (HG+Zn+Ins).

Rabbits in the untreated control and hyperglycemia (HG) groups received daily administration of placebo solution, while rabbits in the HG+Zn, HG+Ins and HG+Zn+Ins groups were commenced on their respective zinc supplementation (Abrisham *et al*., 2010) by oral gavage and insulin therapy (Wang *et al*., 2010) as in Table I.

Table I. Grouping of rabbits and therapeutic interventions.

Group	Description and treatment
UN (n=10)	Rabbits received intravenous injection of normal saline
HG (n=10)	Rabbits received alloxan
HG+Zn (n=10)	Rabbits received alloxan and zinc sulphate (1 ml of 100 mg zinc sulphate /10ml of water for 10 days.)
HG+Ins (n=10)	Rabbits received alloxan and 0.1mg/Kg body weight subcutaneous insulin.
HG+Zn+Ins (n=10)	Rabbits received alloxan and zinc sulphate: Alloxan + 1 ml of 100 mg zinc sulphate /10ml of water for 10 days + 0.1mg/kg Body weight subcutaneous insulin

UN, Untreated; HG, Hyperglyceamia; HG+Zn, Hyperglyceamia and zinc; HG+Ins, Hyperglyceamia and insulin; HG+Zn+Ins, Hyperglyceamia, zinc and insulin.

Alloxan administration

To induce hyperglycemia, a local anesthetic cream (EMLA, Astra Zeneca) was first rubbed onto the dorsal surface of the ear. Then, a preparation of 100 mg/kg b.w alloxan monohydrate (Sigma Aldrich Chemical, Saint Louis, MO, USA) in 4ml sterile normal saline was injected through the marginal ear. Control rabbits were given intravenous injections of saline only. After alloxan administration, 20 % fructose solution was given to the rabbits for a 48-hour period, to avoid possible hypoglycemic shock. The hyperglycemic state was confirmed 48 hours later by measuring blood glucose levels.

Measurement of primary outcome variables.

Fasting blood glucose: Fasting blood glucose was measured at baseline, week 1, week 6 and week 12 with a glucose meter (Performa Accutrend, Roche Diagnostics, Germany). The blood was obtained by lancing the marginal ear vein. A significant increase in glucose baseline value above 100 mg/dl was considered hyperglyceamic (Saleem Mir *et al*., 2015).

Terminal procedures

Animals were euthanized at day 10 after the final administration of therapeutic agents (zinc and/or insulin).

Shortly before euthanasia, rabbits were deeply anesthetized via intramuscular injection of ketamine (50 mg/kg body weight). While under deep anaesthesia, a terminal blood sample was collected via cardiac puncture. Blood was allocated into 4 ml serum-separating tube. Following blood collection, euthanasia was confirmed by administering a lethal overdose of ketamine (100 mg/kg body weight).

The right hemimandible was immediately dissected and fixed in 10 % buffered formalin for subsequent microarchitectural and biomechanical assessments.

For biochemical analysis, blood in serum-separating tubes was centrifuged at 3,000 RPM for 20 min. The resulting serum supernatant was carefully aliquoted and stored at -80 °C until assayed. Serum insulin levels were quantified using a commercial ELISA kit (Elabscience) according to the manufacturer's protocol.

Micro-computed tomography (Micro-CT) acquisition

High-resolution ex vivo the right hemi-mandible was conducted using a Nikon XTH 225/320 LC micro-CT system (Nikon Metrology, UK). Samples were secured within rigid plastic cylindrical holders and stabilized using low-density, radiolucent Styrofoam to minimize motion artefacts and X-ray attenuation. Scanning was performed at a source voltage of 70 kV and a beam current of 400 μA, using a 1 mm aluminium filter to reduce beam hardening. Images were acquired over a 360° rotation with a 1° angular step. The total scan duration per sample was approximately 8 min, yielding a reconstructed isotropic voxel size of 18 μm.

Morphometric analysis

Following volumetric reconstruction, quantitative morphometric analysis was performed using VG Studio Max® 3.2 software (Volume Graphics GmbH, Heidelberg, Germany). In accordance with standard nomenclature (Bouxsein *et al*., 2010), the following parameters were calculated: Bone Volume Fraction (BV/TV), Trabecular Number (TbN), Trabecular Thickness (TbTh), Trabecular Spacing (Tb.Sp), and Cortical Thickness (CtTh). An ellipse a diameter of 2.8 mm, height of 6.8 mm and depth a depth 0.81 mm was taken for the morphometric analysis (Fig. 1 A,B).

Biomechanical assessment (Three-Point Bending)

To evaluate mechanical competence, right hemi mandibles were subjected to three-point bending tests using a universal testing machine (Shimadzu EZ-X S 200V E, Shimadzu South Africa Pty Ltd). The bones were positioned on a support fixture with a span of 13 mm. A compressive load was applied to the mid-diaphysis in the mediolateral plane at a constant displacement rate of 3 mm/min. Load-displacement data were recorded continuously until structural failure occurred.

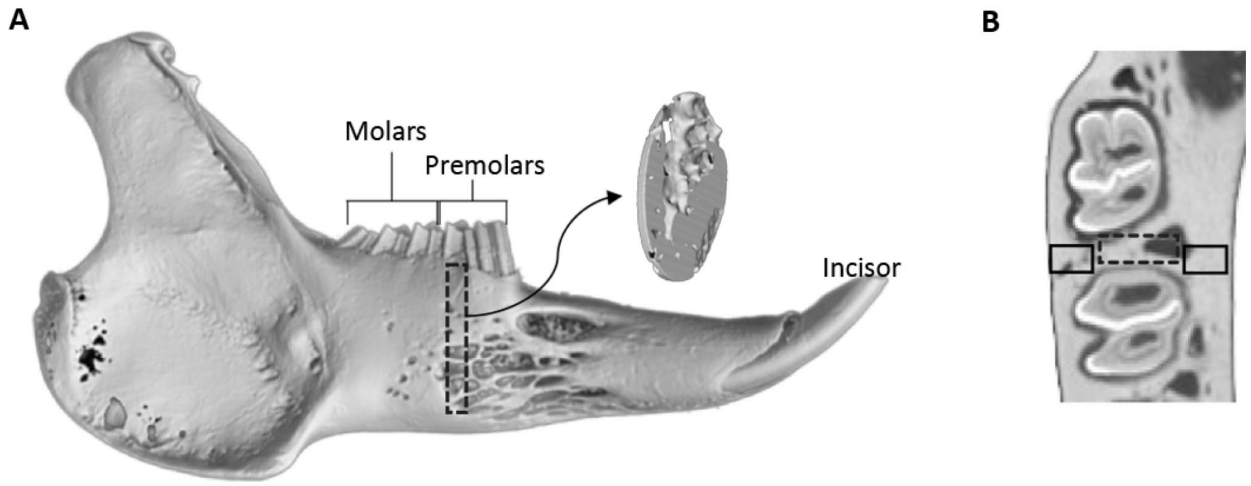

Fig. 1. Micro-Computed Tomography. (A) The dotted line indicates the region of interest (ROI) selected for trabecular morphometric analysis. The inset illustrates the elliptical area positioned between the teeth that were used for the analysis. (B) The same dotted line is shown from a different view for reference. The solid line boxes show the area where cortical thickness measurements were taken.

Statistical analysis

The data obtained were managed in Excel spread sheets (Microsoft Corporation) and analyzed using STATA software Inc (version 16), California. Descriptive statistics of data was done to determine the mean and standard deviation. The test of normality for the data was done using the *Z*-test. Parametric tests were used for normally distributed data while non-parametric tests were used for data not normally distributed. Comparison between the groups was determined using Kruskal–Wallis' test with Dunns's post hoc test as Shapiro Wilks test showed that data were non-parametric. A $p < 0.05$ was considered to be statistically significant.

RESULTS

Fasting blood glucose

At the beginning of the experiment (week 0), there were no significant differences in fasting blood glucose levels between any of the groups ($p>0.05$) (Fig. 2 A). The mean and standard deviation values for week 0 were as follows: UN (67.09±11.27), HG (72.10±12.21), HG+Zn (73.36±12.88), HG+Ins (77.30±8.83), and HG+Zn+Ins (69.36±9.36).

By week 1, significant differences began to emerge. The HG group's mean blood glucose level (149.60±62.60mg/dL) was significantly higher than that of the UN group ($p=0.022$) (Fig. 2 A). All treatment groups showed significantly reduced blood glucose levels compared to the untreated HG group ($p<0.001$for all). The mean and standard deviation for week 1 were: UN (73.82±13.78), HG (149.60±62.60), HG+Zn (133.90±27.32), HG+Ins (122.10±18.67), and HG+Zn+Ins (118.73±16.22).

At the final time point, week 12, the HG group still had a significantly higher mean blood glucose level (146.20±24.12mg/dL) than the UN group ($p<0.001$). The HG+Zn, HG+Ins, and HG+Zn+Ins groups maintained significantly lower blood glucose levels compared to the HG group ($p<0.001$ for each). The mean and standard deviation for week 12 were: UN (72.00±11.56), HG (146.20±24.12), HG+Zn(130.10±22.81), HG+Ins(159.20±32.56), and HG+Zn+Ins(149.45±25.26) (Fig. 2 A).

Serum insulin concentration

The hyperglyceamic group treated with zinc (HG+Zn) (mean=18.43±6.981) and the hyperglyceamic group simultaneously treated with zinc and insulin (HG+Zn+Ins) (mean=17.53±8.556) displayed similar serum insulin levels to the untreated control group (mean=15.16±2.787) ($p=0.557$ and $p=0.638$) (Fig. 2 B). However, the hyperglyceamic group (HG) (mean=34.53±6.417) along with the hyperglyceamic group treated with insulin (HG+Ins) (mean=140.5±153.4) exhibited significantly higher serum insulin values compared to the untreated control ($p=0.001$ and $p=0.018$, respectively).

The serum insulin levels in the HG group were similar to those in the HG+Ins group ($p=0.418$) (Fig. 2 B). However, the HG+Zn and HG+Zn+Ins group had lower serum insulin levels in comparison to the HG group ($p=0.009$ and $p=0.006$, respectively). The HG+Zn group displayed similar serum insulin levels to that of the HG+Ins and HG+Zn+Ins groups ($p=0.076$ and 0.906, respectively). In like manner, the HG+Ins group had similar serum insulin levels to the HG+Zn+Ins ($p=0.058$) (Fig. 2 B).

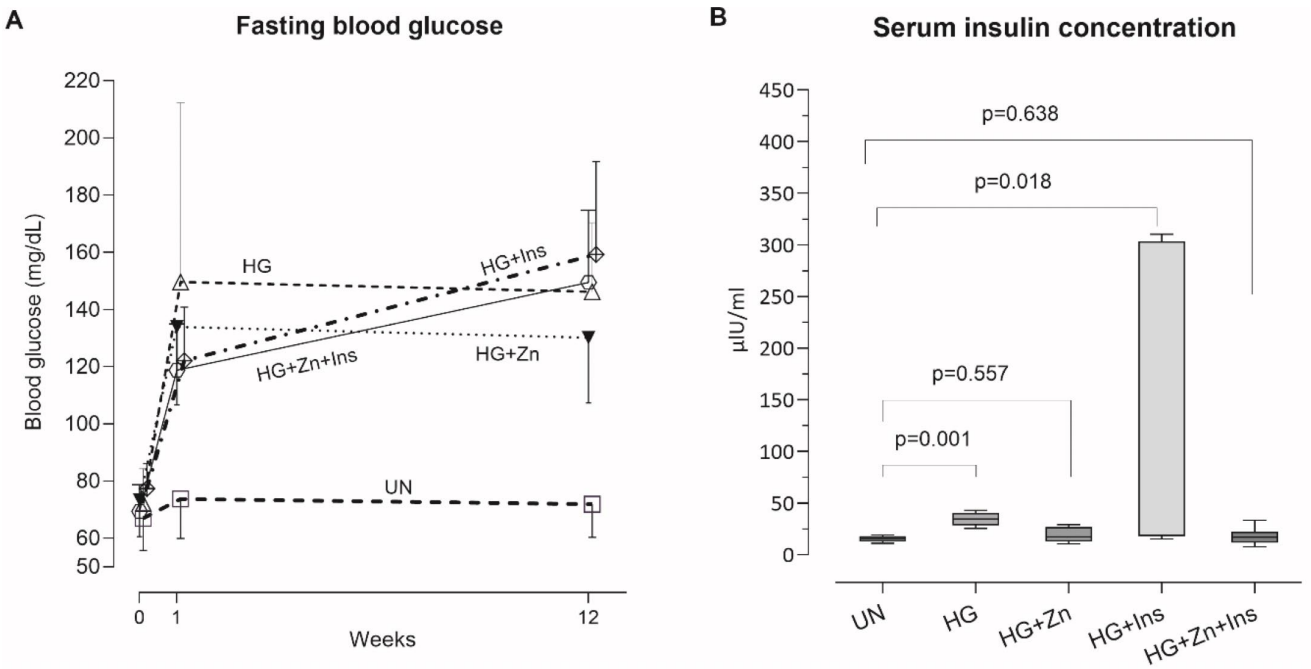

Fig. 2. Blood tests across study groups. (A), Fasting blood glucose levels at baseline (week 0), week 1, and week 12. No significant differences were detected at baseline Hyperglycemic groups showed significantly higher glucose compared to untreated controls at weeks 1 and 12. (B), Serum insulin concentration at termination. Box-and-whisker plots indicate median (line inside box), interquartile range (box), and minimum/maximum values (whiskers). Fasting blood glucose: In week 0, UN *vs.* HG, HG+Zn, HG+Ins, HG+Zn+Ins ($p>0.050$ for all). In week 1 and 12, UN *vs.* HG HG+Zn, HG+Ins, HG+Zn+Ins ($p<0.001$ for all). Serum insulin concentration: HG *vs.* HG+Zn ($p=0.009$), HG+Ins ($p=0.418$), HG+Zn+Ins ($p=0.006$); HG+Zn *vs.* HG+Ins ($p=0.076$), HG+Zn+Ins ($p=0.906$); HG+Ins *vs.* HG+Zn+Ins ($p=0.058$). UN, Untreated; HG, Hyperglyceamia; HG+Zn, Hyperglyceamia and zinc; HG+Ins, Hyperglyceamia and insulin; HG+Zn+Ins, Hyperglyceamia, zinc and insulin

Right mandible biometrics

Maximum force. When compared the UN group, the HG, HG+Zn, HG+Ins and HG+Zn+Ins had similar maximum force ($p=0.545$, $p=0.909$, $p=0.056$ and $p=0.517$, respectively). Similarly, there were no detected differences in maximum force between the HG group and the HG+Zn, HG+Ins and HG+Zn+Ins groups ($p=0.608$, $p=0.244$ and $p=0.991$, respectively). In a similar manner, the HG+Zn group had similar maximum force to the HG+Ins and HG+Zn+Ins groups ($p=0.066$ and $p=0.584$, respectively). The HG+Ins also had similar maximum force to the HG+Zn+Ins group ($p=0.201$).

Break time

When compared to the UN group the break time in the HG, HG+Zn, HG+Ins and HG+Zn+Ins groups was similar ($p=0.520$, $p=0.695$, $p=0.383$ and $p=0.735$, respectively) (Table II). Similarly, when comparing the HG group to the HG+Zn, HG+Ins and HG+Zn+Ins groups there was no significant difference in break time detected ($p=0.311$, $p=0.862$ and $p=0.341$, respectively). This was also the case when comparing the HG+Zn group to the HG+Ins and HG+Zn+Ins groups, no significant differences were detected ($p=0.203$ and $p=0.962$, respectively). The HG+Zn+Ins also displayed similar break time to the HG+Ins group ($p=0.229$) (Table II).

Displacement

When compared to the UN group the displacement in the HG (mean=1.49±0.50), HG+Zn, HG+Ins and HG+Zn+Ins groups was similar ($p=0.526$, $p=0.700$, $p=0.379$ and $p=0.730$, respectively) (Table II). Similarly, when comparing the HG group to the HG+Zn, HG+Ins and HG+Zn+Ins groups there was no significant difference in displacement detected ($p=0.318$, $p=0.849$ and $p=0.342$, respectively) (Table II).

This was also the case when comparing the HG+Zn group to the HG+Ins and HG+Zn+Ins groups, no significant differences were detected ($p=0.203$ and $p=0.973$, respectively). The HG+Zn+Ins also displayed similar displacement to the HG+Ins group ($p=0.224$) (Table II).

Yield point (Force)

The yield point force in the HG (mean=52.84±37.07), HG+Zn (mean=17.77±18.54) and HG+Zn+Ins (mean=10.66±5.23) groups was significantly higher than that on the untreated control group (UN) (mean=5.62±0.44) (p<0.001, for all comparisons) (Table II). However, the HG+Ins group(mean=7.16±1.07) displayed similar yield point force to the UN group (p=0.052).

The HG group had significantly higher yield point force than that of the HG+Ins group (p=0.001) (Table II). Conversely, the HG group had similar yield point force to the HG+Zn and HG+Zn+Ins groups (p=0.430 and p=0.051, respectively). When compared to the HG+Zn group, the HG+Ins group again displayed significantly lower yield point force (p=0.009). While the HG+Zn+Ins group had a similar yield point to the HG+Zn group (p=0.190). Similarly, there was no significant difference in yield point between the HG+Ins and HG+Zn+Ins groups (p=0.197) (Table II).

Table II. Biomechanical properties.

		UN		HG		HG+Zn		HG+Ins		HG+Zn+Ins	
N		10		10		10		10		10	
Maximum force	Mean	166.10	28.69	170.10	62.00	164.10	29.44	202.80	47.94	177.20	45.31
	*p value			0.545		0.909		0.056		0.517	
Break time	Mean	26.83	7.90	29.76	9.97	25.46	7.53	30.16	7.92	25.79	7.78
	*p value			0.52		0.695		0.383		0.735	
Displacement	Mean	1.34	0.40	1.49	0.50	1.27	0.38	1.51	0.40	1.29	0.39
	*p value			0.526		0.7		0.379		0.73	
Yield	Mean	5.62	0.44	42.84	37.07	17.77	18.54	7.16	1.07	10.66	5.29
	*p value			<0.001		<0.001		0.052		<0.001	

Maximum force: HG *vs.* HG+Zn (p=0.608), HG+Ins (p=0.244), HG+Zn+Ins (p=0.991); HG+Zn *vs.* HG+Ins (p=0.066), HG+Zn+Ins (p=0.584); HG+Ins *vs.* HG+Zn+Ins (p=0.201). Break time: HG *vs.* HG+Zn (p=0.311), HG+Ins (p=0.862), HG+Zn+Ins (p=0.341); HG+Zn *vs.* HG+Ins (p=0.203), HG+Zn+Ins (p=0.962); HG+Ins *vs.* HG+Zn+Ins (p=0.229). Displacement: HG *vs.* HG+Zn (p=0.318), HG+Ins (p=0.849), HG+Zn+Ins (p=0.342); HG+Zn *vs.* HG+Ins (p=0.203), HG+Zn+Ins (p=0.973); HG+Ins *vs.* HG+Zn+Ins (p=0.224). Yield: HG *vs.* HG+Zn (p=0.430), HG+Ins (p=0.001), HG+Zn+Ins (p=0.051); HG+Zn *vs.* HG+Ins (p=0.009), HG+Zn+Ins (p=0.190); HG+Ins *vs.* HG+Zn+Ins (p=0.197). * p value for comparison of the UN group with each of the respective groups in the study. UN, Untreated; HG, Hyperglyceamia; HG+Zn, Hyperglyceamia and zinc; HG+Ins, Hyperglyceamia and insulin; HG+Zn+Ins, Hyperglyceamia, zinc and insulin.

Right mandible MicroCT

Bone volume ratio. When compared to the UN control group. the HG and the HG+Zn groups had significantly higher bone volume ratio (p=0.037 and p=0.023, respectively) (Table III). However, the HG+Ins and HG+Zn+Ins groups had similar bone volume ratio when compared to the UN group (p=0.219 and p=0.092, respectively).

When comparing the HG group to the HG+Zn, HG+Ins and HG+Zn+Ins groups there was no significant difference detected (p=0.927, p=0.404 and p=0.679, respectively). In like manner the HG+Zn group had similar bone volume ratio to the HG+Ins and HG+Zn+Ins groups (p=0.336 and p=0.601, respectively). This was also the case for the HG+Ins group when compared to the HG+Zn+Ins group (p=0.674) (Table III).

Trabecular thickness. The UN group had similar trabecular thickness to all the experimental groups; HG, HG+Zn, HG+Ins and HG+Zn+Ins (p=0.445, p=0.800, p=0.823 and p=0.964, respectively) (Table III).

When compared to the HG group, the HG+Zn, HG+Ins and HG+Zn+Ins groups had similar trabecular thickness too (p=0.593, p=0.335 and p=0.429, respectively). Similarly, there no significant differences detected in this regard between the HG+Zn group and both the HG+Ins and HG+Zn+Ins group (p=0.636 and p=0.770, respectively). The same was observed between the HG+Ins group and the HG+Zn+Ins group, there were no significant differences in trabecular thickness (p=0.862) (Table III).

Trabecular number. The UN group had more trabeculae compared to the HG+Zn and the HG+Zn+Ins groups (p=0.010 and p=0.004, respectively). However, the HG (mean=1.17±0.19) and the HG+Ins (mean=1.12±0.10) groups displayed similar number of trabeculae (p=0.174 and p=0.057, respectively) (Table III).

When compared to the HG group, the HG+Zn,

HG+Ins and HG+Zn+Ins groups had similar numbers of trabeculae (p=0.268, p=0.597 and p=0.143). In like manner, the HG+Zn group had similar number of trabeculae when compared to the HG+Ins and HG+Zn+Ins groups (p=0.580 and p=0.672, respectively). The same was true for the trabecular number in HG+Ins group when compared to the HG+Zn+Ins group (p=0.350) (Table III).

Trabecular spacing. The untreated control group (UN) had similar trabecular spacing when compared to the HG+Ins group (p=0.057). However, when compared the HG, HG+Zn and HG+Zn+Ins groups, the UN group had significantly lower trabecular spacing (p=0.026, p=0.002 and p=0.008, respectively) (Table III).

When compared to the HG group, the HG+Zn, HG+Ins and HG+Zn+Ins group had similar trabecular spacing (p=0.512, p=0.750 and p=0.701, respectively). In like manner the HG+Zn group had similar trabeculae spacing when compared to the HG+Ins and HG+Zn+Ins groups (p=0.323 and p=0.799). The same was true for the HG+Ins group when compared to the HG+Zn+Ins group (p=0.482) (Table III).

Cortical thickness. The UN group had significantly larger cortical thickness when compared to the HG, HG+Zn (mean=1.28±0.11), HG+Ins and HG+Zn+Ins groups (p<0.001, p=0.033, p=0.037 and p=0.006, respectively) (Table III).

When compared to the HG group, the HG+Zn, HG+Ins and HG+Zn+Ins groups had similar cortical thickness (p=0.071, p=0.108 and p=0.232, respectively). Similarly, there was no significant difference between the HG+Zn group and the HG+Ins and HG+Zn+Ins groups (p=0.931 and p=0.531, respectively). In like manner, the HG+Ins group had similar cortical thickness to the HG+Zn+Ins (p=0.618) (Table III).

Table III. Trabecular morphometric properties.

		UN		HG		HG+Zn		HG+Ins		HG+Zn+Ins	
N		10		10		10		10		10	
BV/TV	Mean	50.19	8.20	42.20	10.09	40.17	10.74	45.37	10.20	42.20	11.91
	*p value			0.037		0.023		0.219		0.097	
TbTh	Mean	0.40	0.08	0.37	0.09	0.38	0.10	0.41	0.10	0.41	0.11
	*p value			0.445		0.800		0.823		0.964	
TbN	Mean	1.28	0.17	1.17	0.19	1.07	0.18	1.12	0.10	1.04	0.21
	*p value			0.174		0.010		0.057		0.004	
TbSp	Mean	0.39	0.09	0.51	0.13	0.57	0.16	0.49	0.10	0.59	0.23
	*p value			0.026		0.002		0.057		0.008	
CtTh	Mean	1.41	0.04	1.13	0.16	1.28	0.11	1.27	0.14	1.24	0.13
	*p value			P<0.001		0.033		0.037		0.006	

BV/TV: HG *vs.* HG+Zn (p=0.927), HG+Ins (p=0.404), HG+Zn+Ins (p=0.679); HG+Zn *vs.* HG+Ins (p=0.336), HG+Zn+Ins (p=0.601); HG+Ins *vs.* HG+Zn+Ins (p=0.674). TbTh: HG *vs.* HG+Zn (p=0.593), HG+Ins (p=0.335), HG+Zn+Ins (p=0.429); HG+Zn *vs.* HG+Ins (p=0.636), HG+Zn+Ins (p=0.770); HG+Ins *vs.* HG+Zn+Ins (p=0.862). TbN: HG *vs.* HG+Zn (p=0.268), HG+Ins (p=0.597), HG+Zn+Ins (p=0.143); HG+Zn *vs.* HG+Ins (p=0.580), HG+Zn+Ins (p=0.672); HG+Ins *vs.* HG+Zn+Ins (p=0.350). TbSp: HG *vs.* HG+Zn (p=0.512), HG+Ins (p=0.750), HG+Zn+Ins (p=0.701); HG+Zn *vs.* HG+Ins (p=0.323), HG+Zn+Ins (p=0.799); HG+Ins *vs.* HG+Zn+Ins (p=0.482). CtTh: HG *vs.* HG+Zn (p=0.071), HG+Ins (p=0.108), HG+Zn+Ins (p=0.232); HG+Zn *vs.* HG+Ins (p=0.931), HG+Zn+Ins (p=0.531); HG+Ins *vs.* HG+Zn+Ins (p=0.618). *p value for comparison of the UN group with each of the respective groups in the study.
UN, Untreated; HG, Hyperglyceamia; HG+Zn, Hyperglyceamia and zinc; HG+Ins, Hyperglyceamia and insulin; HG+Zn+Ins, Hyperglyceamia, zinc and insulin.

DISCUSSION

This study used an alloxan-induced rabbit model to examine the impact of chronic hyperglycemia, a defining feature of diabetes mellitus, on the integrity of the mandibular bone. Successful induction and maintenance of marked hyperglycemia (serum glucose >100 mg/dL) throughout the experimental period validate this model as a physiologically relevant proxy to investigate skeletal complications associated with

uncontrolled diabetes. Using the intact mandible, the analysis isolates systemic metabolic effects on craniofacial architecture, minimising confounding influences such as active wound healing.

Mechanical properties and the diabetic bone paradox

Mechanical testing did not reveal significant differences in maximum force to failure between the experimental groups. This observation reflects the well-documented 'diabetic bone paradox," wherein individuals with diabetes often exhibit normal or elevated bone mineral density, yet remain highly susceptible to skeletal fragility and fracture (Sharma *et al*., 2024). Such findings reveal the limitations of macroscopic strength metrics in detecting the subtle deterioration in bone material quality characteristic of diabetic skeletopathy (Zhang *et al*., 2025).

In contrast, the yield point analysis provided a more sensitive indicator of compromised material properties (Hernandez & Keaveny, 2006). The markedly higher yield point observed in the hyperglycemic (HG) and zinc-supplemented hyperglycemic (HG+Zn) groups suggests increased stiffness and reduced post-yield ductility, hallmarks of brittle bone. Although advanced glycation end products (AGE) were not quantified in the present study, this mechanical change aligns with literature implicating hyperglycemia-driven non-enzymatic collagen glycation, which promotes pathological crosslinking and alters bone viscoelasticity (Zhang *et al*., 2025). These findings suggest that similar matrix degradation pathways operate within the craniofacial skeleton under sustained hyperglycemic conditions.

Therapeutic outcomes revealed distinct and complex patterns. Zinc monotherapy (HG+Zn) failed to improve mechanical properties compared to untreated hyperglycemic controls, indicating that zinc alone cannot counteract hyperglycemia-induced matrix embrittlement. On the contrary, insulin therapy (HG+Ins) normalised yield point values, consistent with insulin's established anabolic role in bone metabolism (Thrailkill *et al*., 2005), likely through stimulation of remodelling and replacement of compromised matrix (Park *et al*., 2013).

Interestingly, combined zinc and insulin therapy (HG+Zn+Ins) did not produce additive or synergistic benefits. Instead, this group exhibited impaired recovery and trabecular degradation. A plausible explanation involves the dual role in glucose metabolism and insulin signaling. Excessive or poorly timed zinc supplementation under severe hyperglycemia can alter glycemic stability or saturate zinc transport pathways (Fukunaka & Fujitani, 2018), potentially attenuating insulin's anabolic signaling to osteoblasts. This possible 'nutrient signaling conflict' warrants further investigation to optimise dosing and timing in multimodal regimens. While zinc is a known cofactor for alkaline phosphatase and essential for collagen fibrillogenesis, its competitive interaction with insulin in this study suggests a threshold effect (Molenda & Kolmas, 2023). In a state of severe hyperglycemia, the combined demand on cellular transport pathways may lead to saturation, where excess zinc potentially interferes with the anabolic signaling of insulin at the osteoblast receptor level (Fukunaka & Fujitani, 2018). This implies that for neural crest-derived bone, the timing and dosage of zinc are critical, as it may inadvertently act as a secondary stressor rather than a synergetic aid when insulin levels are fluctuating.

Microarchitectural correlates

Micro-CT analysis confirmed systemic reductions in bone volume fraction (BV/TV) in hyperglycemic animals, consistent with insulinopenic diabetic osteopathy characterised by suppressed bone formation due to glucotoxicity and impaired osteoblastogenesis (Thrailkill *et al*., 2005; Abbassy *et al*., 2010; Dlamini & Ndou 2023). Zinc monotherapy did not prevent BV/TV loss, reinforcing its limited efficacy in the absence of insulin. Insulin alone preserved BV/TV, showing its critical role through direct osteoblast receptor signaling (Aeimlapa *et al*., 2018). On the contrary, combined therapy resulted in a degraded trabecular architecture, a decrease in trabecular number (TbN) and increased trabecular separation (TbSp). This mirrors its poor mechanical performance and supporting the hypothesis of a negative pharmacological interaction.

A clinically significant finding was persistent cortical thinning observed in all hyperglycemic groups, including those receiving therapy. This aligns with previous evidence that insulin can mitigate trabecular loss but rarely reverses established cortical deficits (Aeimlapa *et al*., 2018). Irreversibility probably arises due to the fundamental differences in turnover rates as cortical bone has a slower turnover, which makes it vulnerable to lasting damage from early hyperglycemic insults, unlike more easily remodeled spongy bone. Mechanisms such as osteocyte apoptosis, microdamage accumulation, and microvascular compromise can contribute to this persistent deficit (Rosenberg *et al*., 2023). Consequently, cortical thinning can represent a permanent architectural imprint of metabolic injury, perpetuating long-term skeletal fragility even after glycaemic normalisation. This

lack of recovery is particularly significant when considering the mandible's neural crest origin and its intramembranous ossification pathway. Unlike the endochondral bones of the appendicular skeleton, the mandibular cortex relies on a distinct molecular signaling profile that may be more susceptible to early metabolic 'programming' (Lee *et al*., 2001). The fact that cortical thinning remained refractory to therapy suggests that the osteogenic capacity of neural crest-derived cells is uniquely and perhaps permanently altered by initial glucotoxic insults, even when systemic markers are later improved by insulin.

These findings provide a biological explanation for the high rates of dental implant failure and impaired osseous healing observed in diabetic patients (Abbassy *et al*., 2010). Since cortical bone is the primary structure responsible for the mechanical stability of implants, the discovery that cortical thinning is permanent and refractory to insulin therapy is clinically crucial. It suggests that even patients who achieve 'stringent glycaemic control' later in life may still possess a compromised mandibular foundation, necessitating more cautious surgical planning in maxillofacial interventions.

CONCLUSION

This study demonstrates that sustained hyperglycemia inflicts multifaceted damage on the mandible, compromising both the material properties and the microarchitecture in a compartment-specific manner. The study showed that insulin is indispensable for preserving trabecular bone volume and restoring material properties degraded by hyperglycemia. Furthermore, cortical thinning appears to be refractory to therapeutic reversal, suggesting that early skeletal injury may become permanent. The unexpected antagonistic interaction between zinc and insulin underscores the need for mechanistic optimisation of combined therapies. Ultimately, these findings show the paramount importance of early and stringent glycaemic control to prevent irreversible skeletal damage. Future research should focus on elucidating the molecular pathways underlying treatment-resistant cortical deficits and developing strategies for their prevention or mitigation.

ACKNOWLEDGMENTS

We are grateful to the staff of the Multidisciplinary Laboratory for Animal Administration at Obafemi Awolowo University for animal husbandry and the Nuclear Energy Corporation of South Africa (NECSA) for Micro-CT scanning.

OGUNDIPE, O.; PERRY, V.; JAPHTA, N.L.; PILLAY, D. & NDOU, R. Resistencia mandibular y morfología trabecular en conejos hiperglucémicos bajo tratamiento con zinc e insulina. *Int. J. Morphol., 44(3)*:756-765, 2026.

RESUMEN: Las complicaciones diabéticas se originan principalmente por la hiperglucemia crónica, una característica distintiva de la enfermedad cuya prevalencia está aumentando a nivel mundial. Entre estas complicaciones, la afectación esquelética sigue siendo una de las menos estudiadas. Este estudio tuvo como objetivo evaluar el impacto de la hiperglucemia sostenida y las intervenciones terapéuticas con zinc e insulina en la resistencia y la micro arquitectura del hueso mandibular, utilizando un modelo de conejo con hiperglucemia inducida por aloxano. Cincuenta conejos machos fueron asignados aleatoriamente a cinco grupos: control sin tratamiento (UN), hiperglucémico sin tratamiento (HG), hiperglucémico tratado con zinc (HG+Zn), hiperglucémico tratado con insulina (HG+Ins) e hiperglucémico tratado con zinc más insulina (HG+Zn+Ins). La diabetes se indujo con aloxano y los tratamientos se administraron durante 12 semanas. La hemimandíbula derecha se analizó mediante microtomografía computarizada de alta resolución (Micro-CT) y pruebas biomecánicas. Los parámetros morfométricos (BV/TV, TbTh, TbN, TbSp, CtTh) y las propiedades de resistencia mecánica se compararon entre los grupos. La hiperglucemia redujo significativamente la fracción de volumen óseo y el grosor cortical, lo que confirma la vulnerabilidad mandibular a la osteopatía diabética. La fuerza máxima no difirió significativamente entre los grupos. El análisis del punto de fluencia reveló un aumento de la rigidez y la fragilidad en los grupos HG y HG+Zn, mientras que la terapia con insulina normalizó los valores del punto de fluencia. La monoterapia con zinc no logró prevenir el deterioro micro arquitectónico, y la terapia combinada de zinc e insulina afectó inesperadamente la integridad trabecular, lo que sugiere una interacción farmacológica negativa. El adelgazamiento cortical persistente en todos los grupos hiperglucémicos indica déficits estructurales irreversibles a pesar del tratamiento. La insulina es esencial para preservar el hueso trabecular y restaurar las propiedades materiales comprometidas por la hiperglucemia, mientras que el zinc por sí solo no ofrece ningún efecto protector. La falta de sinergia entre el zinc y la insulina demuestra la necesidad de optimizar las terapias combinadas. El control glucémico temprano y estricto sigue siendo fundamental para prevenir el daño esquelético irreversible.

PALABRAS CLAVE: Diabetes mellitus; Hiperglucemia; Mandíbula; Zinc; Insulina; Hueso.

REFERENCES

Abbassy, M. A.; Watari, I. & Soma, K. The effect of diabetes mellitus on rat mandibular bone formation and microarchitecture. *Eur. J. Oral Sci., 118(4)*:364-9, 2010.

Abrisham, S. M.; Yaghmaei, M.; Abbas, F. M.; Sharifi, D. & Abrisham, S. M. Effect of oral zinc therapy on osteogenesis in rabbits. *J. Oral Maxillofac. Surg., 68(7)*:1676-80, 2010.

Adeghate, E.; Schattner, P. & Dunn, E. An update on the etiology and epidemiology of diabetes mellitus. *Ann. N. Y. Acad. Sci., 1084*:1-29, 2006.

Aeimlapa, R.; Charoenphandhu, N.; Suntornsaratoon, P.; Wongdee, K.; Tiyasatkulkovit, W.; Kengkoom, K. & Krishnamra, N. Insulin does not rescue cortical and trabecular bone loss in type 2 diabetic Goto-Kakizaki rats. *J. Physiol. Sci., 68(5)*:531-40, 2018.

Bouxsein, M. L.; Boyd, S. K.; Christiansen, B. A.; Guldberg, R. E.; Jepsen, K. J. & Müller, R. Guidelines for assessment of bone microstructure in rodents using micro-computed tomography. *J. Bone Miner. Res., 25(7)*:1468-86, 2010.

Costantini, S. & Conte, C. Bone health in diabetes and prediabetes. *World J. Diabetes, 10(8)*:421-45, 2019.

Dlamini, G. F. & Ndou, R. Osteoblastogenesis and osteolysis in the Zucker Diabetic Sprague Dawley rat humerus head. *Anat. Cell Biol., 56(4)*:552-61, 2023.

Fukunaka, A. & Fujitani, Y. Role of zinc homeostasis in the pathogenesis of diabetes and obesity. *Int. J. Mol. Sci., 19(2)*:476, 2018.

Hendrijantini, N.; Suisan, Y. C.; Megantara, R. W. A.; Tumali, B. A. S.; Kuntjoro, M.; Ari, M. D. A.; Sitalaksmi, R. M. & Hong, G. Bone remodeling in mandible of Wistar rats with diabetes mellitus and osteoporosis. *Eur. J. Dent., 17(2)*:319-29, 2023.

Hernandez, C. J. & Keaveny, T. M. A biomechanical perspective on bone quality. *Bone, 39(6)*:1173-81, 2006.

Lee, S. K.; Kim, Y. S.; Oh, H. S.; Yang, K. H.; Kim, E. C. & Chi, J. G. Prenatal development of the human mandible. *Anat. Rec., 263(3)*:314-25, 2001.

Leucht, P.; Kim, J. B.; Amasha, R.; James, A. W.; Girod, S. & Helms, J. A. Embryonic origin and Hox status determine progenitor cell fate during adult bone regeneration. *Development, 135(17)*:2845-54, 2008.

Molenda, M. & Kolmas, J. The role of zinc in bone tissue health and regeneration: a review. *Biol. Trace Elem. Res., 201(12)*:5640-51, 2023.

Park, A. G.; Paglia, D. N.; Al-Zube, L.; Hreha, J.; Vaidya, S.; Breitbart, E.; Benevenia, J.; O'Connor, J. P. & Lin, S. S. Local insulin therapy affects fracture healing in a rat model. *J. Orthop. Res., 31(5)*:776-82, 2013.

Rosenberg, J. L.; Woolley, W.; Elnunu, I.; Kamml, J.; Kammer, D. S. & Acevedo, C. Effect of non-enzymatic glycation on collagen nanoscale mechanisms in diabetic and age-related bone fragility. *Biocell, 47(7)*:1651-9, 2023.

Saleem Mir, M.; Maqbool Darzi, M.; Khalil Baba, O.; Khan, H. M.; Kamil, S. A.; Sofi, A. H. & Wani, S. A. Streptozotocin induced acute clinical effects in rabbits (*Oryctolagus cuniculus*). *Iran. J. Pathol., 10(3)*:206-13, 2015.

Sharma, P.; Sharma, R. K. & Gaur, K. Understanding the impact of diabetes on bone health: a clinical review. *Metabol. Open, 24*:100330, 2024.

Sun, H.; Saeedi, P.; Karuranga, S.; Pinkepank, M.; Ogurtsova, K.; Duncan, B. B.; Stein, C.; Basit, A.; Chan, J. C. N.; Mbanya, J. C.; *et al*. IDF Diabetes Atlas: global, regional and country-level diabetes prevalence estimates for 2021 and projections for 2045. *Diabetes Res. Clin. Pract., 183*:109119, 2022.

Thrailkill, K. M.; Lumpkin, C. K., Jr.; Bunn, R. C.; Kemp, S. F. & Fowlkes, J. L. Is insulin an anabolic agent in bone? Dissecting the diabetic bone for clues. *Am. J. Physiol. Endocrinol. Metab., 289(5)*:E735-45, 2005.

Walle, M.; Whittier, D. E.; Frost, M.; Müller, R. & Collins, C. J. Meta-analysis of diabetes mellitus-associated differences in bone structure assessed by high-resolution peripheral quantitative computed tomography. *Curr. Osteoporos. Rep., 20(6)*:398-409, 2022.

Wang, J.; Wan, R.; Mo, Y.; Zhang, Q.; Sherwood, L. C. & Chien, S. Creating a long-term diabetic rabbit model. *Exp. Diabetes Res., 2010*:289614, 2010.

Wu, B.; Fu, Z.; Wang, X.; Zhou, P.; Yang, Q.; Jiang, Y. & Zhu, D. A narrative review of diabetic bone disease: characteristics, pathogenesis, and treatment. *Front. Endocrinol. (Lausanne), 13*:1052592, 2022.

Zhang, Y.; Zhang, Z.; Tu, C.; Chen, X. & He, R. Advanced glycation end products in disease development and potential interventions. *Antioxidants (Basel), 14(4)*:492, 2025.

Corresponding author:
Robert Ndou
Department of Human Anatomy and Histology
School of Medicine
Sefako Makgatho Health Sciences University
Molotlegi Str.
Ga-Rankuwa
Pretoria 0204
SOUTH AFRICA

E-mail: Robert.Ndou@smu.ac.za